

An adaptive element subdivision technique for evaluating 3D weakly singular boundary integrals

J. Zhang, C. Lu, Y. Zhong, G. Xie & Y. Dong

*State Key Laboratory of Advanced Design and Manufacturing
for Vehicle Body, Hunan University, China*

Abstract

A general adaptive element subdivision technique is presented for the numerical evaluation of weakly singular integrals, which often appear in three-dimensional boundary element analysis equations. In this algorithm, the weakly singular boundary element is broken up into a few sub-elements through a sphere of decreasing radius. The sub-elements involving the singular point are evaluated numerically after using a coordinate transformation to remove the singularities, while other quadrilateral sub-elements and triangular sub-elements are evaluated numerically by the standard Gaussian quadrature and Hammer quadrature respectively. The number of sub-elements and their size are determined adaptively according to the position of the singular point. Numerical examples are presented for both planar and curved surface element. The results demonstrate our method can provide higher accuracy and efficiency than the conventional method.

Keywords: weakly singular integrals, 3D boundary element, subdivision techniques, Gaussian quadrature.

1 Introduction

Weakly singular integrals are appeared in the basic boundary integral equations (BIEs) when the boundary integral equation method (BEM) is used to solve potential and mechanical problems. Accurate evaluating weakly singular integral is of importance for successful implementation of BEM. Much effort has been made to remove the weakly singular integrals arising in BIEs. Chati and



Mukherjee have used a method suggested by Nagaranjan and Mukherjee [1] to carry out the weakly singular integration in boundary node method. Usually, polar coordinate transformation is used to solve this problem [2]. Zhang proposed a new coordinate transformation denoted as (α, β) transformation to deal with weakly singular integrals [3]. However, due to the reason of conventional polar coordinate transformation and (α, β) transformation just by directly connecting the singular point with each vertex of element, shape of sub-elements will be poor when the singular point is located near the edge or in the edge etc., which will result in poor calculation accuracy. The (α, β) transformation is similar to the polar coordinate transformation. However, its implementation is simpler than that of polar transformation.

In this paper, an adaptive element subdivision technique is presented by dividing the boundary element over which the source point is located into a number of sub-elements through a sphere of decreasing radius. This algorithm is similar to the advancing Front method [4] which should update vertex and edge in every step. No matter where the position of the source point is located, every sub-element has relative good shape with the proposed algorithm. Then the (α, β) transformation is used to remove singularities in the sub-element which includes the source point. While the remaining regular quadrilateral and triangular sub-elements are respectively evaluated using the standard Gaussian quadrature and Hammer quadrature. The computational results show that higher accuracy could be obtained even with fewer Gaussian points. A number of element subdivision and numerical examples are given to verify the presented method.

2 3D singular boundary integrals

In this paper, we deal with the following boundary integral with weakly singularity over 3D boundary element S :

$$I = \int_S \frac{f(y, r)}{r} \phi(x) dS(x) \quad (1)$$

where y and x are referred to as the source point and the field point in BEM, respectively, y is in S , r is the Euclidean distance between y and x , f is a well-behaved function, and $\phi(x)$ is a shape function. Since y is inside the integration element S , the integrals (1) become weakly singular.

Now, we consider the boundary integral equations of 3D potential problems in the domain Ω enclosed by the boundary Γ . The basic function is presented in terms of the potential u on the boundary as follows [5]:

$$c(y)u(y) = \int_{\Gamma} q(x)u^*(x, y)d\Gamma(x) - \int_{\Gamma} u(x)q^*(x, y)d\Gamma(x) \quad (2)$$

where c is a coefficient depending on the smoothness of the boundary at the source point y . $u^*(x, y)$ is the fundamental solution for the 3D problem expressed as

$$u^*(x, y) = \frac{1}{4\pi} \frac{1}{r(x, y)} \quad (3)$$

And $q^*(x, y)$ is the derived fundamental solutions

$$q^*(x, y) = \frac{\partial u^*(x, y)}{\partial n} \quad (4)$$

where n is the unit outward normal direction to the boundary Γ , with components $n_i, i = 1, 2, 3$.

To numerically evaluate boundary integrals for Eqs. (2), the boundary Γ is divided into a number of surface elements. Then boundary integration is performed on each element as Eqs. (1). Weakly singular integrals arise when the source point is inside the integration element.

In this paper, we develop an adaptive element subdivision technique coupled with the (α, β) transformation for weakly singular integrals on 3D boundary element. The detailed implementation is described in the following section.

3 Adaptive element subdivision technique

To further improve the computational accuracy of the weakly singular integral, an adaptive element subdivision technique is proposed in this part. With this adaptive element subdivision technique, no matter where the position of the source point is located in the element, good shape of sub-elements could be obtained due to the property of sphere and merging operation. Since this subdivision technique is performed in element local coordinate space, it is a uniform algorithm for every kind element. Here we take quadrilateral element as an example to explain the algorithm. The detailed procedure is introduced as follows:

Definition 1:

For a 3D boundary element which the source point is located in, let Dpt_{source} be the position of source point. V_i^t and E_i^t are referred to as its vertex and corresponding edge respectively. R_i^t is the line segment starting from Dpt_{source} and ending with V_i^t as shown in Fig. 1, $i=0, 1, 2$ if it's a triangular element, or $i=0, 1, 2, 3$ if it's a quadrilateral element at the beginning of procedure, subsequently, the number of i is indefinite due to the update of procedure, V_i^t and E_i^t are arranged by counterclockwise, where t is the number of step and it's ended with the condition which will be mentioned as follows.

Definition 2:

Let l_{max} be the maximum distance from Dpt_{source} to V_i^t and l_{minVtx} be the minimum distance from Dpt_{source} to V_i^t where Dpt_{source} is not coincident with V_i^t , let $l_{minEdge}$ be

the minimum distance from Dpt_{source} to E_i^t where Dpt_{source} is not located in E_i^t . Then we define l_{min} as:

$$l_{min} = \min \{l_{minVtx}, l_{minEdge}\} \quad (5)$$

In every step, a sphere with the center of Dpt_{source} is constructed and its radius defined as:

$$r_{sphere} = ratio^t * l_{max} \quad (6)$$

If $r_{sphere} < ratioMin * l_{min}$, sub-elements without containing the source point are obtained as shown in Fig. 2, otherwise the sub-elements including the source point are obtained, where $ratioMin$ and $ratio$ are empirical value. The sphere may be intersected with E_i^t and R_i^t , as shown in Fig. 1, let $Irad_i^t$ be the intersection point between R_i^t and the sphere, let $IFir_i^t$ and $ISec_i^t$ be the first and second intersection points between R_i^t and the sphere.

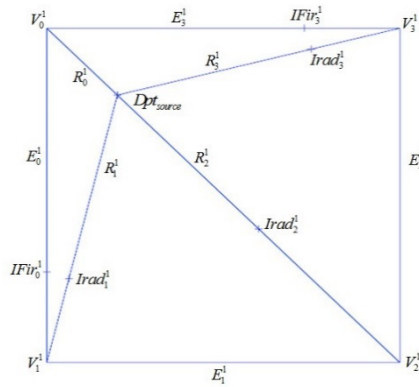


Figure 1: First step of element subdivision.

In order to simplify the algorithm, the detailed operations for updating V_i^t and E_i^t will be omitted. The main algorithm for creating sub-element is described by pseudo-code format in Table 1.

Table 1: Creating sub-element algorithm.

```

for each edge  $E_i^t$ 
  if ( $V_i^t$  in the sphere)
    if ( $IFir_i^t \parallel ISec_i^t$ )
      if ( $IFir_i^t$ )
        a new triangular sub-element is created
        with  $IFir_i^t, V_{Next}^t, IRad_{Next}^t$ 
      end

```

Table 1: Continued.

```

        if(  $IFir_i^t \ \&\& \ ISec_i^t$  )
            a new triangular sub-element is created
            with  $ISec_i^t, V_{Next}^t, Irad_{Next}^t$ 
        end
    end
else
    if(  $IFir_i^t \parallel ISec_i^t$  )
        if(  $IFir_i^t$  )
            a new triangular sub-element is created
            with  $V_i^t, IFir_i^t, Irad_i^t$ 
        end
        if(  $IFir_i^t \ \&\& \ ISec_i^t$  )
            a new triangular sub-element is created
            with  $ISec_i^t, V_{Next}^t, Irad_{Next}^t$ 
        end
    else
        a new quadrilateral sub-element is created
        with  $ISec_i^t, V_{Next}^t, Irad_{Next}^t$ 
    end
end
end
Where  $V_{Next}^t, Irad_{Next}^t$  are the corresponding next item of  $i$  in  $t$  step.

```

As shown in Fig. 2, after above procedure, new sub-elements have been obtained and V_i^t and E_i^t have also been updated, then repeat the algorithm until all sub-elements have been created.

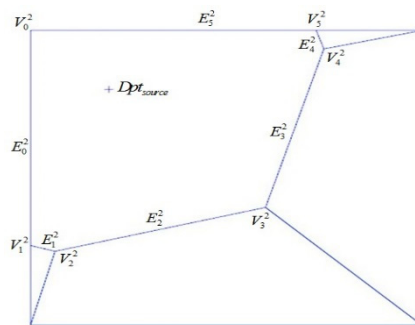


Figure 2: Second step of element subdivision.

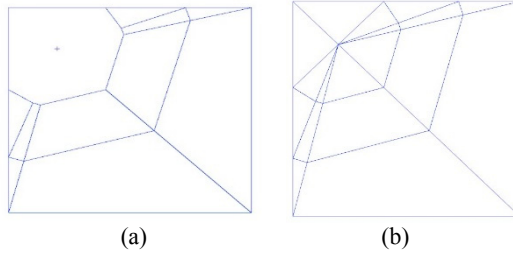


Figure 3: Element subdivision before merging operation.

There are two factors that influence the computational accuracy of (α, β) transformation for sub-element which includes the source point. One is that length of the two edges intersecting with the source point of the sub-element can't be much difference, another is that angle between the two edge can't be too large. If second case occurred, then sub-element will be divided into two sub-elements again until angle of every sub-element satisfied the condition $angle < diviAngle$ defined in the procedure. As shown in Fig. 3(b), although the length of the two edges of the sub-element is same and the angle is small enough, which is beneficial for (α, β) transformation to obtain more accurate results, total number of sub-elements is too large which will cause much more computational cost and shape of some of sub-element without including the source point have relative poor which will cause accuracy problems. In order to deal with this situation, a merging operation will be introduced. If $IFir_i^t$ is close to V_i^t or V_{Next}^t defined as $d(IFir_i^t, V_i^t) < edgeFactor * d(V_i^t, V_{Next}^t)$ or $d(IFir_i^t, V_{Next}^t) < edgeFactor * d(V_i^t, V_{Next}^t)$, $edgeFactor = 0.1$, then move the $IFir_i^t$ to V_i^t or V_{Next}^t , which is similar to $ISec_i^t$.

If $Irad_i^t$ is close to $IFir_i^t$ or V_i^t defined as $d(Irad_i^t, IFir_i^t) < radFactor * r_{sphere}$ or $d(Irad_i^t, V_i^t) < radFactor * r_{sphere}$, $radFactor = 0.1$, then move the $Irad_i^t$ to $IFir_i^t$ or V_i^t . New sub-elements can be obtained after merging operation as shown in Fig. 4. The number of sub-elements is reduced and shape of sub-elements is improved apparently.

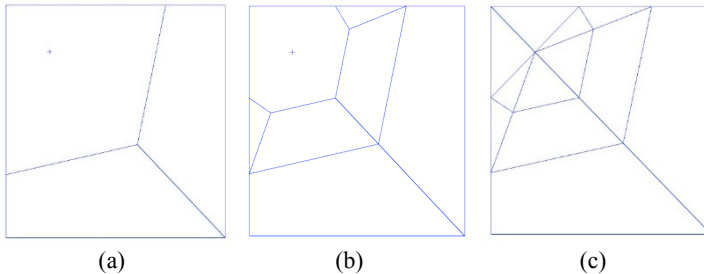


Figure 4: Element subdivision after merging operation.

There are some advantages of the proposed adaptive element subdivision technique. In this method, the sub-elements including the source point have better shape than that in conventional subdivision method [3], while the remaining sub-elements also have better shape due to the property of sphere and merging operation. The second is that more Gaussian points are shifted towards the source point and a large number of Gaussian points are avoided compared to the conventional subdivision method which will be mentioned in next section. What's more, the number of sub-elements and their size are determined adaptively by the position of singular point. Using the adaptive element subdivision technique coupled with the (α, β) transformation, the weakly singular integrals can be calculated with higher accuracy. The reader should note that all the intersecting points should be projected from real-world coordinate space to element local coordinate space in this algorithm.

4 Numerical examples

In this section, comparison between the adaptive element subdivision and conventional subdivision are made. In the conventional subdivision method, the integration element is divided directly into sub-triangles by simply connecting the singular point with each vertex of element as shown in Fig. 5, thus the shape of sub-triangles will poor when the singular point is located near the edge or in the edge especially for slender elements, which will result in the numerical results become less accurate [6, 7]. However, with the proposed adaptively element subdivision technique, integration element is broken up into triangular and quadrilateral sub-elements through a sphere of decreasing radius, consequently, shape of sub-element is good which are beneficial conditions for using (α, β) transformation to get more accuracy.

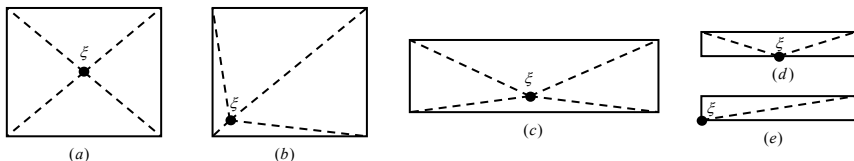


Figure 5: The conventional subdivisions of quadrilateral element.

Several examples of element subdivision and corresponding numerical examples compared with conventional subdivision method for planar element and curved surface element are presented to verify the effectiveness and accuracy of our method. The position of vertices of the element is labeled in the corresponding picture and numerical result comparison is presented in the table following element subdivision examples. In order to better compare our method with conventional method, the same integral scheme is used in numerical examples. The (α, β) transformation is used to remove singularities in the sub-element

which includes the source point. While the remaining regular quadrilateral and triangular sub-elements are respectively evaluated by the standard Gaussian quadrature and Hammer quadrature. In this paper, $ratioMin = \sqrt{2}$, $ratio = 0.25$, the numerical values obtained by our method and conventional method named as sphere subdivision and direct subdivision respectively will be compared to ‘exact’ values in terms of the relative error defined by:

$$\text{Relative Error} = \left| \frac{I_{numerical} - I_{exact}}{I_{exact}} \right| \quad (7)$$

where $I_{numerical}$ and I_{exact} are the numerical and ‘exact’ values of the integral under consideration, respectively. The accuracy of I_{exact} is to 13 decimal places.

4.1 Planar element examples

In these examples, adaptive element subdivision and corresponding numerical result are presented for planar rectangular element with the node coordinates of (1, 1), (-1, 1), (-1, -1), (1, -1) as shown in Fig. 6 and slender element with the node coordinates of (10, 1), (0, 1), (0, 0), (10, 0) as shown in Fig. 7. The coordinates of the source points are set at (0.99, 0.9), (0.0, 0.99), (9.0, 0.9), (5.0, 0.9). The figure on the right with red box is the partial enlarged view of the corresponding figure on the left as shown in Fig. 6 and Fig. 7. Total number of Gaussian points and Relative Error of numerical evaluation for planar rectangular and slender element with two different subdivision method are listed in Table 2. As shown in Fig. 6 and Fig. 7, shape of sub-elements of planar rectangular element and slender element are good with the proposed adaptive element subdivision technique.

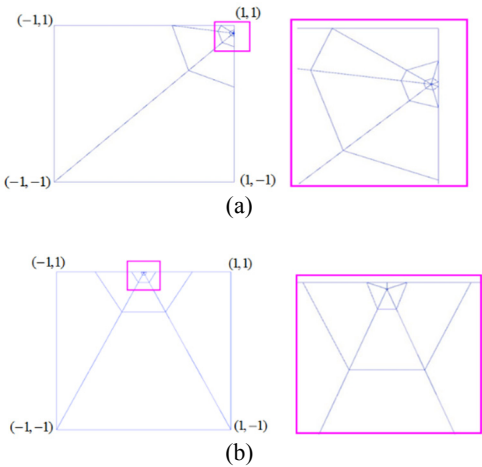


Figure 6: The sphere adaptive subdivisions of planar rectangular element.

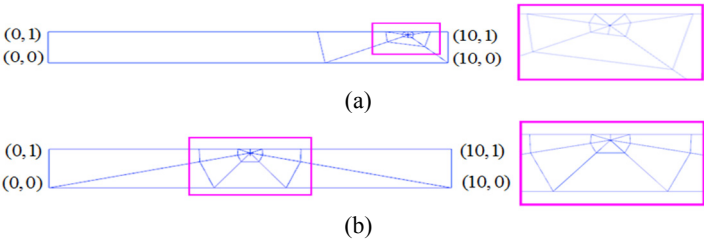


Figure 7: The sphere adaptive subdivisions of planar slender element.

Table 2: Numerical evaluation for planar rectangular element and slender element.

Planar element	Source point	Gaussian points number		Relative error	
		direct subdivision	sphere subdivision	direct subdivision	sphere subdivision
rectangular	(0.99, 0.9)	1200	1191	4.46e-004	7.73e-008
	(0.0, 0.99)	1200	843	2.10e-003	3.35e-008
slender	(9.0,0.9)	1200	1100	3.73e-004	2.73e-007
	(5.0, 0.9)	1200	1100	3.55e-003	8.18e-008

4.2 Curved surface element examples

In these examples, adaptive element subdivision and corresponding numerical result are presented for curved surface rectangular element with the node coordinates of (1, 1, 1), (-1, 1, 0), (-1, -1, 1), (1, -1, 0) as shown in Fig. 8 and slender element with the node coordinates of (10, 1, 0.5), (0, 1, 0), (0, 0, 0.5), (10, 0, 0) as shown in Fig. 9. The figure on the right is the planform of the corresponding figure on the left and the figure on the below is its partial enlarged view as shown in Fig. 8 and Fig. 9. The coordinates of the source points are set at (0.99, 0.9, 0.9455), (0.0, 0.99, 0.5), (9.5, 0.95, 0.4525), (5.0, 0.9, 0.25). Total number of Gaussian points and Relative Error of numerical evaluation for curved surface rectangular and slender element with two different subdivision methods are listed in Table 3. As shown in Fig. 8 and Fig. 9, shape of sub-elements of curved surface rectangular element and slender element are good with the proposed adaptive element subdivision technique.

The results demonstrate that shape of sub-elements for planar or curved surface element is good with the proposed adaptive element subdivision technique and our method can provide higher accuracy and efficiency than the conventional method even with fewer Gaussian points.

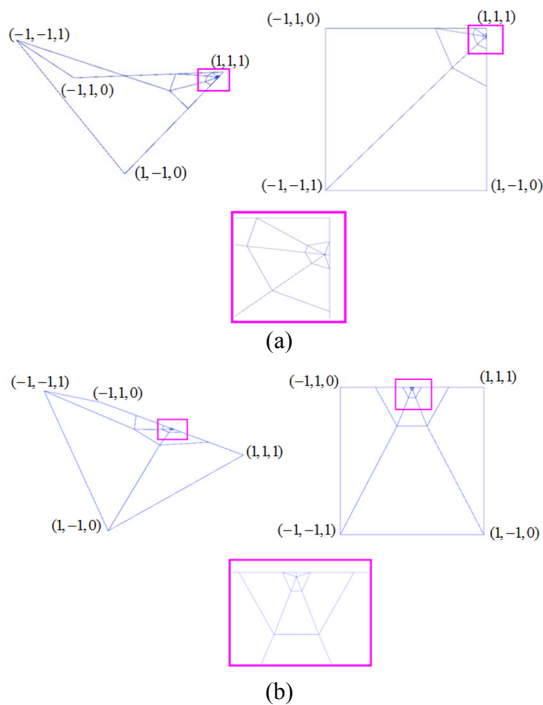


Figure 8: The sphere adaptive subdivisions of curved rectangular element.

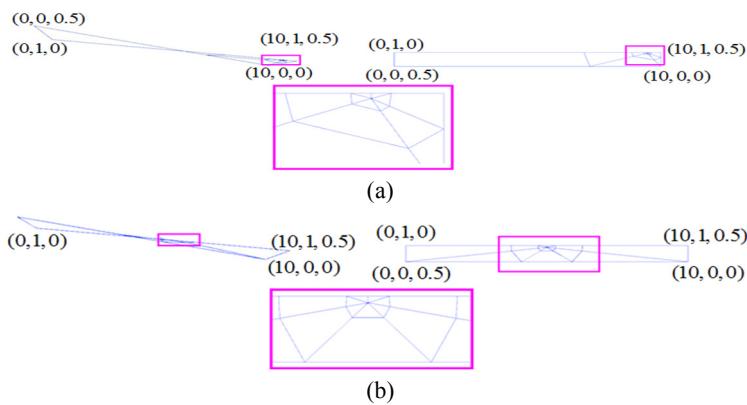


Figure 9: The sphere adaptive subdivisions of curved slender element.

Table 3: Numerical evaluation for curved surface rectangular and slender element.

Curved surface element	Source point	Gaussian points number		Relative error	
		direct subdivision	sphere subdivision	direct subdivision	sphere subdivision
rectangular	(0.99,0.9,0.9455)	1200	815	5.74e-004	2.13e-007
	(0.0, 0.99,0.5)	1200	843	2.33e-003	8.44e-009
slender	(9.5,0.95,0.4525)	1200	1045	1.28e-003	1.74e-007
	(5.0, 0.9,0.25)	1200	1100	3.50e-003	8.63e-008

5 Conclusions and future work

A general adaptive element subdivision technique for the numerical evaluation of weakly singular integrals on 3D boundary element was proposed in this paper. Employing the proposed method, no matter planar and curved surface boundary element or where the position of singular point is located, sub-elements with good shape can be obtained which is convenient for getting higher accuracy. This algorithm is simple and powerful. Numerical examples were presented to verify our method. Results demonstrated that with this adaptive element subdivision algorithm higher accuracy and efficiency can be obtained than the conventional method. Extension of our work to 3D nearly singular integral is under consideration now.

Acknowledgements

This work was supported in part by National Science Foundation of China under grant number 11172098, in part by Hunan Provincial Natural Science Foundation for Creative Research Groups of China under grant number 12JJ7001, in part by Open Research Fund of Key Laboratory of High Performance Complex Manufacturing, Central South University under grant number Kfkt2013-05 and in part by Hunan Provincial Innovation Foundation for Postgraduate under grant number CX2013B150.

References

- [1] Nagarajan A, Mukherjee S. A mapping method for numerical evaluation of two-dimensional integrals with $1/r$ singularity [J]. Computational mechanics, 1993, 12(1-2): 19-26.
- [2] Klees R. Numerical calculation of weakly singular surface integrals [J]. Journal of Geodesy, 1996, 70(11): 781-797.
- [3] Zhang J, Qin X, Han X, *et al*. A boundary face method for potential problems in three dimensions [J]. International journal for numerical methods in engineering, 2009, 80(3): 320-337.
- [4] Wu B, Wang S. Automatic triangulation over three-dimensional parametric surfaces based on advancing front method [J]. Finite elements in analysis and design, 2005, 41(9): 892-910.



- [5] Ma H, Kamiya N. Distance transformation for the numerical evaluation of near singular boundary integrals with various kernels in boundary element method [J]. Engineering analysis with boundary elements, 2002, 26(4): 329-339.
- [6] Xie G, Zhou F, Zhang J, *et al.* New variable transformations for evaluating nearly singular integrals in 3D boundary element method [J]. Engineering Analysis with Boundary Elements, 2013, 37(9): 1169-1178.
- [7] Qin X, Zhang J, Xie G, *et al.* A general algorithm for the numerical evaluation of nearly singular integrals on 3D boundary element [J]. Journal of computational and applied mathematics, 2011, 235(14): 4174-4186.

